

Colloidal Synthesis of Single-Layer MSe_2 ($M = Mo, W$) Nanosheets via Anisotropic Solution-Phase Growth Approach

Wonil Jung,[†] Sujeong Lee,[†] Dongwon Yoo,[†] Sohee Jeong,[†] Pere Miró,[‡] Agnieszka Kuc,[‡] Thomas Heine,[‡] and Jinwoo Cheon^{*,†}

[†]Department of Chemistry, Yonsei University, Seoul 120-749, Korea

[‡]Department of Physics and Earth Science, Jacobs University Bremen, 28759 Bremen, Germany

S Supporting Information

ABSTRACT: The generation of single-layer 2-dimensional (2D) nanosheets has been challenging, especially in solution-phase, since it requires highly anisotropic growth processes that exclusively promote planar directionality during nanocrystal formation. In this study, we discovered that such selective growth pathways can be achieved by modulating the binding affinities of coordinating capping ligands to the edge facets of 2D layered transition-metal chalcogenides (TMCs). Upon changing the functional groups of the capping ligands from carboxylic acid to alcohol and amine with accordingly modulated binding affinities to the edges, the number of layers of nanosheets is controlled. Single-layer MSe_2 ($M = Mo, W$) TMC nanosheets are obtained with the use of oleic acid, while multilayer nanosheets are formed with relatively strong binding ligands such as oleyl alcohol and oleylamine. With the choice of appropriate capping ligands in the 2D anisotropic growth regime, our solution-based synthetic method can serve a new guideline for obtaining single-layer TMC nanosheets.

Recently, single-layer sheets of van der Waals (vdW) transition-metal chalcogenides (TMCs), in which single layers are held together by vdW force,¹ have emerged as uniquely important nanostructures with unprecedented materials properties, analogous to graphene.² These single-layer TMCs exhibit remarkable materials characteristics when compared to their multilayer bulk counterpart. For example, when group VI TMC nanomaterials become thinned to the single layer, the electronic structure of indirect band gap in the bulk changes to direct band gap with enhanced optoelectronic transitions.³ In addition, the excellent in-plane charge carrier mobility and giant spin-valley coupling are some of the electronic characteristics that can enable the high-performance capabilities of optoelectronic and spintronic devices.⁴

During the past decade, solution methods have been demonstrated as one of the most powerful synthetic approaches for a wide range of nanostructures composed of covalent-networks between metals and chalcogens,⁵ including 0-dimensional (0D) quantum dots, 1-dimensional (1D) nanowires, and 2-dimensional (2D) nanosheets.⁶ For example, CdSe nanocrystals have been successfully synthesized in a size- and shape-controlled fashion from spheres^{6a,b} to platelets^{6e,f} and branched complex structures.^{6d} Even with such synthetic advances, one of

the current challenges is the lack of proper synthetic protocols for free-standing single-layer 2D nanosheets of vdW TMCs.⁷ According to the recent studies, even though solution-based synthetic methods have provided some glimpse on the formation of single-layer TMCs in the early stage of growth processes,⁸ multilayered TMCs are typically isolated as stable products.⁹ One most recent study shows that controlled delivery of chalcogen source during the crystal growth processes is critical to generate single layers of group IV TMCs such as TiS_2 , ZrS_2 , and HfS_2 .¹⁰ Even with these studies, the understanding and the control of growth processes for single-layer TMC nanosheets are still elusive, not to mention the lack of reliable synthetic protocols.

In this study, we demonstrate a colloidal methodology for single-layer nanosheets of MSe_2 ($M = Mo, W$) by exclusively promoting their anisotropic lateral growth mode. We discovered that the use of specific surface capping ligands with different binding energies to the reactive edge facets of TMCs is the most important factor to produce thickness-controlled TMCs from multi- to single-layer. The strength of ligand binding to the given crystallographic facet is theoretically examined to understand the ligand-dependent anisotropic growth modes. While the roles of capping ligands on the anisotropic growth effects for other 0D and 1D nanostructures are well-known, this is the first demonstration of capping ligand-driven synthetic protocol for single-layer nanosheets of vdW TMCs.

As a representative case of our study, we first chose WSe_2 . Each layer of WSe_2 is weakly bonded by vdW force and comprises a Se–W–Se triatomic layer where tungsten (W) is covalently bonded to six selenium (Se) atoms in a trigonal prismatic geometry (Figure 1a).¹¹ WSe_2 nanosheets are synthesized by reacting tungsten hexacarbonyl ($W(CO)_6$) and diphenyl diselenide (Ph_2Se_2) in the presence of capping ligand as a solvent (Figure 1b).¹² We tested three different types of capping ligands (i.e., oleylamine, oleyl alcohol, and oleic acid) having the same number of carbon atoms, but different terminal functional groups. $W(CO)_6$ (0.02 mmol) is reacted with Ph_2Se_2 (0.04 mmol) in the excess amount of capping ligand (14 mmol) at 330 °C under an Ar atmosphere. After 12 h, the reaction mixture is cooled down and centrifuged to isolate WSe_2 nanosheets with high colloidal stability when dispersed in nonpolar solvents such as toluene (Figure S2). According to our DFT calculations, such

Received: March 16, 2015

Published: June 8, 2015

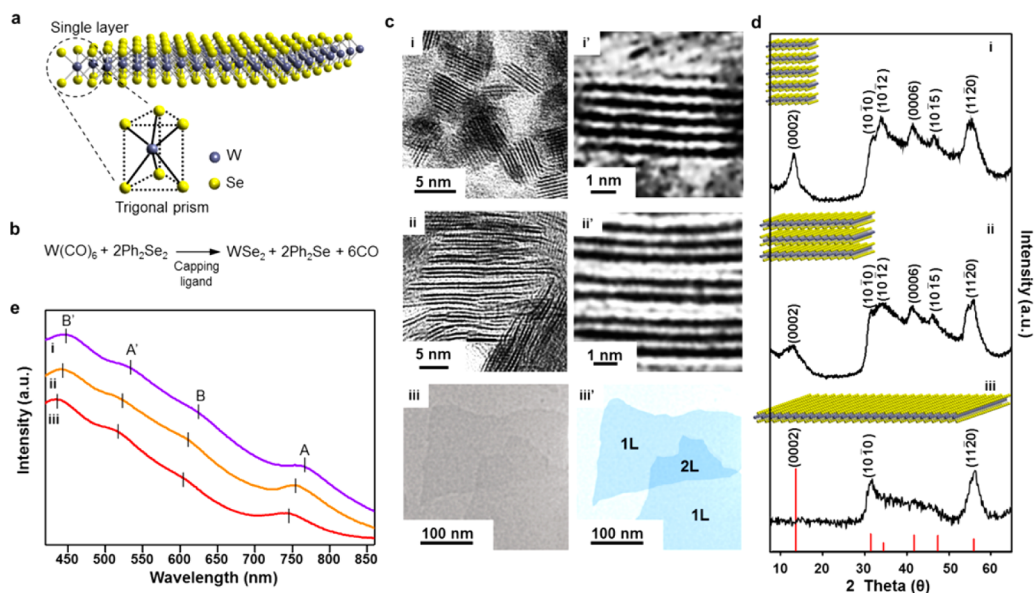


Figure 1. Lateral size- and thickness-controlled synthesis of WSe₂ nanosheets with the use of different capping ligands. (a) Visualization of single-layer WSe₂ and its trigonal prism geometry with ball-and-stick model. (b) Chemical equation for WSe₂ nanosheets. (c) TEM images of WSe₂ nanosheets synthesized with (i) oleylamine, (ii) oleyl alcohol, and (iii) oleic acid. (i', ii') Magnified TEM images of the nanosheets, and (iii') pseudocolor image of the single-layer nanosheets. (d) XRD patterns of WSe₂ nanosheets synthesized with (i) oleylamine, (ii) oleyl alcohol, and (iii) oleic acid. (e) UV-vis absorption spectra of WSe₂ nanosheets synthesized with (i) oleylamine (purple line), (ii) oleyl alcohol (orange line), and (iii) oleic acid (red line).

high solubility is presumably due to the presence of weak vdW interaction between the capping ligands and the solvent (Table S2). In the case of oleylamine, 4–8 layered WSe₂ nanosheets with a lateral size of ~5 nm are obtained (Figure 1c(i),(i')). This result is consistent with previous synthetic studies on group VI WS₂ and WSe₂ nanosheets where multiple sheets are formed when alkyl amines such as oleylamine or dodecylamine are used.^{8,13} When the capping ligand is changed to oleyl alcohol, the lateral size of the WSe₂ nanosheets is increased to ~21 nm and the number of layers is reduced to 2 or 3 (Figure 1c(ii),(ii')). Finally, oleic acid affords single-layer WSe₂ nanosheets with a larger lateral size of 200–400 nm (Figure 1c(iii),(iii')). Figure 1d shows the XRD patterns of WSe₂ nanosheets obtained by the three different types of capping ligands indexed to the reflections of bulk WSe₂ (red bars, JCPDS 38-1388). The gradual decline of the (0002) reflection of the *c*-axis takes place as the thickness of the WSe₂ nanosheets decreases, and the (0002) peak is not observed in the single-layer WSe₂ nanosheets. In UV-vis absorption spectra of the WSe₂ nanosheets with different number of layers, blue-shift of excitonic peaks, such as A, B, A', and B', are observed as the thickness is reduced to single layer (Figure 1e). For example, an excitonic peak A, which arises from direct gap transitions at the K point, is blue-shifted from 766 nm (4–8 layers) to 753 nm (2–3 layers) and 743 nm (1 layer). The observed thickness dependency of excitonic peak positions is in good agreement with previous findings.¹⁴

The single-layer WSe₂ nanosheets obtained by this synthetic approach using oleic acid as the capping ligand are further examined. Figure 2a shows a transmission electron microscopy (TEM) image of WSe₂ nanosheets with a lateral size of 200–400 nm, and a pseudocolor image of the selected area exhibits single-layer nanosheets with some overlap between them (Figure 2b). Time-dependent TEM study reveals that initially generated small (~3 nm) plate-like particles, generated within a few minutes, continuously grow in lateral direction to 200–400 nm over the 12 h time span (Figure S3). High-resolution TEM image for the top-view of the nanosheets shows a regular atomic arrangement

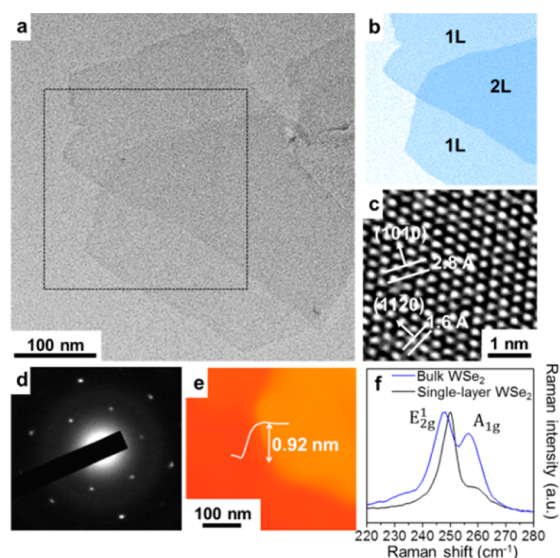


Figure 2. Single-layer WSe₂ nanosheets. (a) Low-magnification TEM image and (b) pseudocolor image of the selected area in the box of panel a. (c) High-resolution TEM image, (d) SAED pattern, and (e) AFM image of a single-layer WSe₂ nanosheet. (f) Raman spectra of bulk WSe₂ (blue line) and single-layer WSe₂ (black line).

and lattice fringes of hexagonal patterns, along the direction of (10 $\bar{1}$ 0) and (11 $\bar{2}$ 0), which correspond to the *d*-spacing of 2.8 and 1.6 Å, respectively (Figure 2c). Selected area electron diffraction (SAED) pattern for the single-layer WSe₂ nanosheets certifies their single crystallinity (Figure 2d). Atomic force microscopy (AFM) confirms the presence of nanosheets with a thickness of ca. 0.92 nm (Figure 2e), which indicates single-layer WSe₂.¹⁵ Raman spectroscopy is a sensitive technique to monitor the formation of single-layer TMCs. While two distinct peaks in the Raman spectra of in-plane E_{2g}¹ and out-of plane A_{1g} are observed at 248 and 256 cm⁻¹, respectively, for bulk WSe₂, there is a clear

peak shift of the E_{2g}^1 mode to 250 cm^{-1} along with a peak intensity decrement of the A_{1g} mode upon the formation of the single layer (Figure 2f), which is consistent with previous reports.¹⁶

Binding affinities of the capping ligands play a key role in altering the anisotropic growth pattern of WSe_2 nanosheets, as observed in the experiments. Such phenomenon can be examined by the binding energy difference in the capping ligands, which is the energy required to attach one capping ligand to a specific facet.¹⁷ Employing density functional theory (DFT, for computational details see Supporting Information (SI)), we calculated the binding energies of three simplified capping ligands (i.e., methylamine, methyl alcohol, and formic acid) with the $(10\bar{1}0)$ and $(11\bar{2}0)$ facets, which are the representative edge facets of WSe_2 nanosheets (Figure 3 and S1).¹⁸ The use of

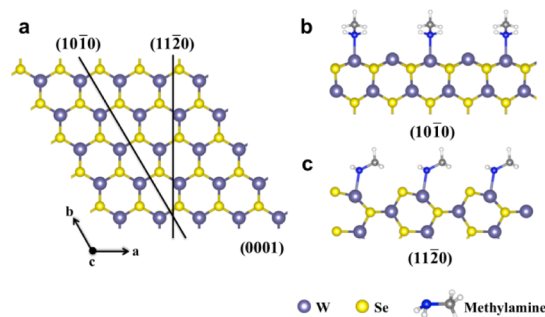


Figure 3. Structure model of the WSe_2 basal plane viewed from the top. (a) The $(10\bar{1}0)$ and $(11\bar{2}0)$ cutting planes are shown with black lines. Ligand binding models for methylamine to the (b) $(10\bar{1}0)$ and (c) $(11\bar{2}0)$ WSe_2 edge facets, as viewed from the (0001) basal plane.

simplified ligand model for our calculation is based on the fact that the binding energy between the capping ligands and the nanosheets significantly differs by their functional groups, while the contribution from chain length is minor to generate critical information for interpretation of the synthetic experimental results.

Capping ligands bind to the metal center, and the binding energies to the $(10\bar{1}0)$ edge are -1.475 , -1.161 , and -0.848 eV for methylamine, methyl alcohol, and formic acid, respectively, which indicates that methylamine has the most favorable binding interaction, while formic acid shows the least (Table 1). Similarly,

Table 1. Calculated Binding Energies of Three Different Capping Ligands to Edge Facets of WSe_2 at the PBE-D3-BJ/TZP Level of Theory

capping ligand	binding energy ^a (eV)	
	$(10\bar{1}0)$	$(11\bar{2}0)$
methylamine	-1.475	-1.421
methyl alcohol	-1.161	-0.978
formic acid	-0.848	-0.780

$$^a E_{\text{binding}} = E_{\text{facet-ligand}} - E_{\text{facet}} - E_{\text{ligand}}$$

the trend of ligand binding energies to the $(11\bar{2}0)$ edge is consistent with the one observed for the $(10\bar{1}0)$ edge (Table 1). Such results indicate that strongly bound capping ligands (i.e., oleylamine) stabilize the edge facets and inhibit lateral growth, while vertical growth of WSe_2 nanosheets will competitively occur, leading to smaller but multilayered nanosheets. On the contrary, oleic acid with a significantly less stabilizing effect to the edge facets facilitates the lateral anisotropic growth, and

eventually single-layer WSe_2 nanosheets are formed. Such binding energy difference of capping ligands is well-correlated with electron-donating ability of the ligands to the metal center in the order of amine, alcohol, and carboxylic acid.¹⁹

Our solution synthetic method is further extended to single-layer nanosheets of MoSe_2 . A mixture of molybdenum hexacarbonyl ($\text{Mo}(\text{CO})_6$, 0.02 mmol) and Ph_2Se_2 (0.04 mmol) with the use of a capping ligand of oleic acid, is heated up to $350\text{ }^\circ\text{C}$, and the reaction is maintained for 10 h. After workup process of centrifugation, single-layer MoSe_2 nanosheets with a lateral size of 200–500 nm are obtained as shown in the TEM image (Figure 4a). An area is selected to show a clear

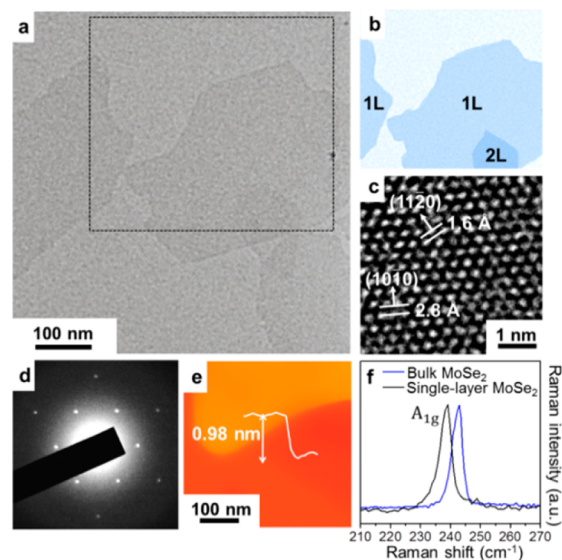


Figure 4. Single-layer MoSe_2 nanosheets. (a) Low-magnification TEM image and (b) pseudocolor image of the selected area in the box of panel a. (c) High-resolution TEM image, (d) SAED pattern, and (e) AFM image of a single-layer MoSe_2 nanosheet. (f) Raman spectra of bulk MoSe_2 (blue line) and single-layer MoSe_2 (black line).

contrast between a single layer and a stacked area with a pseudocolor image (Figure 4b). The top-view of high-resolution TEM image shows a repeated atomic arrangement of lattice fringes with the d -spacing of 2.8 and 1.6 Å for the $(10\bar{1}0)$ and $(11\bar{2}0)$ hexagonal planes of the single-layer MoSe_2 nanosheets (Figure 4c). SAED pattern of the single-layer MoSe_2 nanosheets confirms their single crystallinity (Figure 4d). AFM shows the thickness of a MoSe_2 nanosheet (Figure 4e) with a measured height of ca. 0.98 nm, which verifies that the product is single-layer nanosheets. For Raman spectral analysis, the A_{1g} mode of single-layer MoSe_2 is shifted to 239 cm^{-1} from 242 cm^{-1} for bulk MoSe_2 , which is also consistent with the previous observation (Figure 4f).²⁰ The XRD pattern of the single-layer MoSe_2 nanosheets exhibits no peaks related to c -axis (Figure S4). Similar to WSe_2 , UV-vis absorption spectra of single-layer MoSe_2 nanosheets show an excitonic peak A at 790 nm, which is higher energy compared to the bulk MoSe_2 (Figure S5).

In this study, we discovered that in order to have solution growth for single-layer 2D nanosheets of TMCs, modulation of the surface energy with the use of proper capping ligands is important. The functional groups of the capping ligands with different coordinating strengths can shift the growth mode from the exclusive lateral mode of single-layer nanosheets to mixed modes of both lateral and vertical growth for multilayer

nanosheets. Therefore, once suitable capping ligands for promoting selective lateral directions are found, our approach could be extended to a wide range of single-layer 2D nanosheets.

■ ASSOCIATED CONTENT

■ Supporting Information

Detailed theoretical methods. The Supporting Information is available free of charge on the ACS Publications website at DOI: 10.1021/jacs.5b02772.

■ AUTHOR INFORMATION

Corresponding Author

*jcheon@yonsei.ac.kr

Notes

The authors declare no competing financial interest.

■ ACKNOWLEDGMENTS

This work was financially supported by the National Creative Research Initiatives of Korea (2010-0018286), the Asian Office of Aerospace Research and Development (FA2386-14-1-0014), and Deutsche Forschungsgemeinschaft (DFG HE 3543/18-1). We thank Dr. Chi Won Ahn at Korea National Nanofab Center for supporting the AFM analysis.

■ REFERENCES

- (1) (a) Huang, X.; Zeng, Z.; Zhang, H. *Chem. Soc. Rev.* **2013**, *42*, 1934. (b) Eda, G.; Yamaguchi, H.; Voiry, D.; Fujita, T.; Chen, M.; Chhowalla, M. *Nano Lett.* **2011**, *11*, 5111. (c) Tongay, S.; Zhou, J.; Ataca, C.; Lo, K.; Matthews, T. S.; Li, J.; Grossman, J. C.; Wu, J. *Nano Lett.* **2012**, *12*, 5576. (d) Li, H.; Wu, J.; Yin, Z.; Zhang, H. *Acc. Chem. Res.* **2014**, *47*, 1067.
- (2) (a) Butler, S. Z.; Hollen, S. M.; Cao, L.; Cui, Y.; Gupta, J. A.; Gutierrez, H. R.; Heinz, T. F.; Hong, S. S.; Huang, J.; Ismach, A. F.; Johnston-Halperin, E.; Kuno, M.; Plashnitsa, V. V.; Robinson, R. D.; Ruoff, R. S.; Salahuddin, S.; Shan, J.; Shi, L.; Spencer, M. G.; Terrones, M.; Windl, W.; Goldberg, J. E. *ACS Nano* **2013**, *7*, 2898. (b) Song, I.; Park, C.; Choi, H. C. *RSC Adv.* **2015**, *5*, 7495. (c) Huang, J.-K.; Hsu, C.-L.; Chiu, M.-H.; Juang, Z.-Y.; Chang, Y.-H.; Chang, W.-H.; Iwasa, Y.; Takenobu, T.; Li, L.-J. *ACS Nano* **2014**, *8*, 923. (d) Eda, G.; Fujita, T.; Yamaguchi, H.; Voiry, D.; Chen, M.; Chhowalla, M. *ACS Nano* **2012**, *6*, 7311. (e) Miró, P.; Audiffred, M.; Heine, T. *Chem. Soc. Rev.* **2014**, *43*, 6537. (f) Lebègue, S.; Björkman, T.; Klintonberg, M.; Nieminen, R. M.; Eriksson, O. *Phys. Rev. X* **2013**, *3*, 031002. (g) Tan, C.; Zhang, H. *Chem. Soc. Rev.* **2015**, *44*, 2713. (h) Huang, X.; Tan, C.; Yin, Z.; Zhang, H. *Adv. Mater.* **2014**, *26*, 2185. (i) Zeng, Z.; Yin, Z.; Huang, X.; Li, H.; He, Q.; Lu, G.; Boey, F.; Zhang, H. *Angew. Chem., Int. Ed.* **2011**, *50*, 11093.
- (3) (a) Splendiani, A.; Sun, L.; Zhang, Y.; Li, T.; Kim, J.; Chim, C. Y.; Galli, G.; Wang, F. *Nano Lett.* **2010**, *10*, 1271. (b) Mak, K. F.; Lee, C.; Hone, J.; Shan, J.; Heinz, T. F. *Phys. Rev. Lett.* **2010**, *105*, 136805. (c) Kuc, A.; Zibouche, N.; Heine, T. *Phys. Rev. B* **2011**, *83*, 245213. (d) Yin, Z.; Li, H.; Li, H.; Jiang, L.; Shi, Y.; Sun, Y.; Lu, G.; Zhang, Q.; Chen, X.; Zhang, H. *ACS Nano* **2012**, *6*, 74.
- (4) (a) Radisavljevic, B.; Radenovic, A.; Brivio, J.; Giacometti, V.; Kis, A. *Nat. Nanotechnol.* **2011**, *6*, 147. (b) Wang, Q. H.; Kalantar-Zadeh, K.; Kis, A.; Coleman, J. N.; Strano, M. S. *Nat. Nanotechnol.* **2012**, *7*, 699. (c) Ross, J. S.; Wu, S.; Yu, H.; Ghimire, N. J.; Jones, A. M.; Aivazian, G.; Yand, J.; Mandrus, D. G.; Xia, D.; Yao, W.; Xu, X. *Nat. Commun.* **2013**, *4*, 1474. (d) Larentis, S.; Fallahzad, B.; Tutuc, E. *Appl. Phys. Lett.* **2012**, *101*, 223104. (e) Podzorov, V.; Gershenson, M. E.; Kloc, C.; Zeis, R.; Bucher, E. *Appl. Phys. Lett.* **2004**, *84*, 3301. (f) Kappera, R.; Voiry, D.; Yalcin, S. E.; Branch, B.; Gupta, G.; Mohite, A. D.; Chhowalla, M. *Nat. Mater.* **2014**, *13*, 1128. (g) Lin, L.; Xu, Y.; Zhang, S.; Ross, I. M.; Ong, A. C. M.; Allwood, D. A. *ACS Nano* **2013**, *7*, 8214. (h) Zhu, Z. Y.; Cheng, Y. C.; Schwingenschlöggl, U. *Phys. Rev. B* **2011**, *84*, 153402.
- (5) (a) Yin, Y.; Alivisatos, A. P. *Nature* **2005**, *437*, 664. (b) Jun, Y.-w.; Choi, J.-s.; Cheon, J. *Angew. Chem., Int. Ed.* **2006**, *45*, 3414. (c) Jun, Y.-

- w.; Lee, J.-H.; Choi, J.-s.; Cheon, J. *J. Phys. Chem. B* **2005**, *109*, 14795. (d) Liu, Y.; Wu, Z.; Zhang, H. *Adv. Colloid Interface Sci.* **2014**, *207*, 347.
- (6) (a) Dabbousi, B. O.; Rodriguez-Viezo, J.; Mikulec, F. V.; Heine, J. R.; Mattoussi, H.; Jensen, R. K. F.; Bawendi, M. G. *J. Phys. Chem. B* **1997**, *101*, 9463. (b) Pradhan, N.; Reifsnnyder, D.; Xie, R.; Aldana, J.; Peng, X. *J. Am. Chem. Soc.* **2007**, *129*, 9500. (c) Orendorff, C. J.; Gearheart, L.; Jana, N. R.; Murphy, C. J. *J. Phys. Chem. Chem. Phys.* **2006**, *8*, 165. (d) Kumar, S.; Nann, R. *Small* **2006**, *3*, 316. (e) Ithurria, S.; Tessier, M. D.; Mahler, B.; Lobo, R. P. S. M.; Dubertret, B.; Efros, A. L. *Nat. Mater.* **2011**, *10*, 936. (f) Son, J. S.; Wen, X.-D.; Joo, J.; Chae, J.; Baek, S.-I.; Park, K.; Kim, J. H.; An, K.; Yu, J. H.; Kwon, S. G.; Choi, S.-H.; Wang, Z.; Kim, Y.-W.; Kuk, Y.; Hoffmann, R.; Hyeon, T. *Angew. Chem., Int. Ed.* **2009**, *48*, 6861.
- (7) Chen, J.; Wu, X.-J.; Yin, L.; Li, B.; Hong, X.; Fan, Z.; Chen, B.; Xue, C.; Zhang, H. *Angew. Chem., Int. Ed.* **2015**, *54*, 1210.
- (8) (a) Altavilla, C.; Sarno, M.; Ciambelli, P. *Chem. Mater.* **2011**, *23*, 3879. (b) Seo, J.-w.; Jun, Y.-w.; Park, S.-w.; Nah, H.; Moon, T.; Park, B.; Kim, J.-G.; Kim, Y. J.; Cheon, J. *Angew. Chem., Int. Ed.* **2007**, *46*, 8828. (c) Park, K. H.; Choi, J.; Kim, H. J.; Oh, D.-H.; Ahn, J. R.; Son, S. U. *Small* **2008**, *4*, 945.
- (9) (a) Mahler, B.; Hoepfner, V.; Liao, K.; Ozin, G. A. *J. Am. Chem. Soc.* **2014**, *136*, 14121. (b) Jeong, S.; Yoo, D.; Jang, J.-t.; Kim, M.; Cheon, J. *J. Am. Chem. Soc.* **2012**, *134*, 18233. (c) Jang, J.-t.; Jeong, S.; Seo, J.-w.; Kim, M.-C.; Sim, E.; Oh, Y.; Nam, S.; Park, B.; Cheon, J. *J. Am. Chem. Soc.* **2011**, *133*, 7636. (d) Sekar, P.; Greyson, E. C.; Barton, J. E.; Odom, T. W. *J. Am. Chem. Soc.* **2005**, *127*, 2054. (e) Zhou, X.; Jiang, J.; Ding, T.; Zhang, J.; Pan, B.; Zuo, J.; Yang, Q. *Nanoscale* **2014**, *6*, 11046.
- (10) Yoo, D.; Kim, M.; Jeong, S.; Han, J.; Cheon, J. *J. Am. Chem. Soc.* **2014**, *136*, 14670.
- (11) (a) Chhowalla, M.; Shin, H. S.; Eda, G.; Li, L.-J.; Loh, K. P.; Zhang, H. *Nat. Chem.* **2013**, *5*, 263. (b) Wilson, A.; Yoffe, A. D. *Adv. Phys.* **1969**, *18*, 193.
- (12) Trace amount of tetradecylphosphonic acid is simultaneously used as an additive, which prevents the formation of WO₃ during the reaction.
- (13) Antunez, P. D.; Webber, D. H.; Brutchey, R. L. *Chem. Mater.* **2013**, *25*, 2385.
- (14) (a) Zhao, W.; Ghorannevis, Z.; Chu, L.; Toh, M.; Kloc, C.; Tan, P. H.; Eda, G. *ACS Nano* **2013**, *7*, 791. (b) Consadori, F.; Frindt, R. F. *Phys. Rev. B* **1970**, *2*, 4893. (c) Crowne, F. J.; Amani, M.; Birdwell, A. G.; Chin, M. L.; O'Regan, T. P.; Najmaei, S.; Liu, Z.; Ajayan, P. M.; Lou, J.; Dubey, M. *Phys. Rev. B* **2013**, *88*, 235302.
- (15) Zheng, J.; Zhang, H.; Dong, S.; Liu, Y.; Nai, C. T.; Shin, H. S.; Jeong, H. Y.; Liu, B.; Loh, K. P. *Nat. Commun.* **2014**, *5*, 2995.
- (16) (a) Zeng, H.; Liu, G. B.; Dai, J.; Yan, Y.; Zhu, B.; He, R.; Xie, L.; Xu, S.; Chen, X.; Yao, W.; Cui, X. *Sci. Rep.* **2013**, *3*, 1608. (b) Zhao, W.; Ghorannevis, Z.; Amara, K. K.; Pang, J. R.; Toh, M.; Zhang, X.; Kloc, C.; Tan, P. H.; Eda, G. *Nanoscale* **2013**, *5*, 9677.
- (17) (a) Manna, L.; Wang, L. W.; Cingolani, R.; Alivisatos, A. P. *J. Phys. Chem. B* **2005**, *109*, 6183. (b) Rempel, J. Y.; Trout, B. L.; Bawendi, M. G.; Jensen, K. F. *J. Phys. Chem. B* **2006**, *110*, 18007. (c) Spirko, J. A.; Neiman, M. L.; Oelker, A. M.; Klier, K. *Surf. Sci.* **2003**, *542*, 192.
- (18) (a) Le, D.; Rahman, T. S. *J. Phys.: Condens. Matter* **2013**, *25*, 312201. (b) Botello-Méndez, A. R.; López-Urías, F.; Terrones, M.; Terrones, H. *Nanotechnology* **2009**, *20*, 325703. (c) Jiang, J. W.; Zhuang, X.; Rabczuk, T. *Sci. Rep.* **2013**, *3*, 2209.
- (19) Hinze, J.; Jaffé, H. H. *J. Am. Chem. Soc.* **1962**, *84*, 540.
- (20) (a) Tonndorf, P.; Schmidt, R.; Böttger, P.; Zhang, X.; Börner, J.; Leibig, A.; Albrecht, M.; Kloc, C.; Gordan, O.; Zahn, D. R. T.; de Vasconcelos, S. M.; Bratschitsch, R. *Opt. Express* **2013**, *21*, 4908. (b) Ramakrishna Matte, H. S. S.; Plowman, B.; Datta, R.; Rao, C. N. R. *Dalton Trans.* **2011**, *40*, 10322.